Pore scale investigation of dopants impact on wettability alteration

Franck Nono[1,2,*], *Titly Farhana Faisal*[1], *Florent Fischer*[1], *Fabrice Pairoys*[1], *Mohamed Regaieg*[1], and *Cyril Caubit*[1]

[1]TotalEnergies, CSTJF, Avenue Larribau, 64000 Pau, France
[2]Akkodis, 4 Rue Jules Ferry, 64000 Pau, France

Abstract. Wettability is a key parameter controlling fluid flow in porous media as it affects the fluids pore space distribution thus the outcoming flow properties such as capillary pressure and relative permeability. Experiments imaged with micro-CT scanner have enabled the observation of pore scale flow mechanisms and thus helped to implement the relevant physics in pore scale simulators. They were also used to provide an estimation of rock/fluids properties such as wettability. For instance, Regaieg et al (2022,2023) have used DRP experiments to anchor pore scale simulation and provided a predictive workflow for relative permeability that was applied for homogenous permeable sandstones.

It is a common practice in DRP experiments to use dopants in brine/oil to enhance the contrast between fluids and optimize image processing. However, a recent experimental study on outcrop sandstones achieved by TotalEnergies SCAL laboratory (Pairoys et al., 2023) highlighted significant differences in wettability alteration when using a doped brine during the ageing step in comparison to experiments with non-doped brine. These findings question the usage of dopants in DRP experiments and highlight the importance of estimating the dopants impact on DRP laboratory protocols.

In this study, we conducted 2 different Amott-like experiments on the same reservoir sandstones: i) In the first experiment we used the old Amott-like protocol as presented in Regaieg et al., 2022, using an adapted doped brine and a crude oil to perform the wettability test including ageing, (ii) In the second experiment, we modified the ageing step by using a non-doped formation brine. Micro-computed tomography was used to compare the results of both experiments at the pore scale. We focused our observations on 5 main aspects: (i) Average saturation and saturation profiles, (ii) Pore occupancies, (iii) Capillary rise rates, (iv) Trapping, (v) flow properties at residual saturations. Our study shows that there are significant differences in both experiments even though the same wettability pattern is conserved. We observed that the dopants tend to render water-wet pores more water-wet than the experiments without dopants, thus in line with the SCAL observation. In contrast, computed Amott-like indices suggest a less water-wet behavior when using the doped formation brine. A caution is made here on the trapping that occurs during the spontaneous steps that may have important implications on our general understanding of these indices. The experiment with the new protocol provided different simulation wettability input and made the DRP workflow more robust.

1. Introduction

Digital Rock Physics has prevailed over the past 20 years as an emerging technique enabling the understanding of complex pore-scale multiphase flow phenomena that are impossible to visualize with conventional devices. Very recently, [1, 2] developed an entire workflow merging fast DRP experiments with pore network simulations (PNM) to predict relative permeabilities within a shorter timeline compared to SCAL experiments. The authors managed to overcome the two main bottlenecks that hindered the DRP community from providing such a predictive and fast workflow for many years. One of them relied on how accurately we could provide reliable wettability distribution in the pore network. A wettability anchoring experiment was designed using the basis from the known SCAL Amott wettability experiment. The main additional benefit from DRP is the direct visualization of the pore occupancies during the different steps.

Micro-CT visualizations are possible if there is a good contrast between the different fluids present in the pore network. Typical formation brines and dead oil have very low contrast on 3D X-ray images. It is very common to add dopants in one of the fluids (mainly in brine) to enhance the contrast. Sodium Iodide or potassium iodide are the most used brine dopants. However, some studies highlighted the possible impact of adding dopants on wettability alteration [3,4,5]. Very recently, Pairoys et al. [6] conducted an insightful SCAL experimental investigation of dopants effect on spontaneous imbibition dynamic and residual oil saturation. The authors used different NaI (Sodium iodide) brine salinities, a dead oil, Bentheimer outcrops and different aging strategies. It turned out that increasing dopants concentration in brine increased spontaneous imbibition rate thus the water-wetness of water-wet pores. The residual oil saturations also increased. One key observation was that if the ageing step is performed with non-doped connate brine, spontaneous imbibition and residual oil saturation are not impacted even if a doped brine is used in the later stages of

* Corresponding author: franck.nono@totalenergies.com

the Amott wettability experiment. These observations raised an important issue regarding the DRP experimental protocols and the reliability of our designed wettability anchoring experiment to predict relative permeabilities.

The objective of this paper is to assess the impact of using NaI on wettability alteration at the pore scale thus on DRP wettability outputs. For this purpose, our comparisons will be based on an experimental design similar to the wettability anchoring experiment that was proposed by Regaieg et al. [1, 2]. This wettability anchoring experiment was designed to feed pore network simulation with specific pore occupancy statistics and some experimental measurements. For example, the authors used 2 weeks of spontaneous displacements as it was found to be sufficient to have enough statistics to provide to the model. But this previous (old) experimental design included using the doped brine throughout the experiment, including during ageing.

To take into consideration the observations made by Pairoys et al. [6], we designed a new wettability anchoring experiment in which the connate brine during ageing does not contain dopants. The previous "old" ([2]) and the new wettability anchoring experiments are then applied on the same reservoir rock with same initial wettability (water-wet). Results show significant differences, emphasizing the need to upgrade DRP wettability characterization protocols.

2. Materials and methods

2.1. Porous media

The reservoir rock used for tests has a semi-unconsolidated structure, primarily composed of quartz grains (see **Table 1**). It is classified as having a poorly sorted coarse sand structure, with a mean grain size distribution around 630 µm and a median value around 550 µm. The peak of the pore-throat radius size distribution obtained via MICP test is around 20 µm (see Figure 1), making this reservoir rock suitable for DRP investigations.

Table 1. Mineralogy of the reservoir rock used in this study.

Mineralogy	**92.4% Quartz** – **5.7% Feldspar** – 1.8% Clays & Micas – 0.1% Others

For this study, we used a mini plug with a diameter of 10 mm and a length of 15 mm. The measured absolute permeability is 4.65D +/- 0.4D. Permeability is measured twice, at 100% full mineral oil saturation and at 100% full brine saturation. Explanations of the importance of these steps are given in paragraph **2.4**. To measure permeability, 8 different ranges of flowrates are imposed, and the resulted equilibrium pressure gradients are acquired. One-phase flow Darcy formula considering gravity is used to calculate the absolute permeability. Very accurate Rosemount® pressure sensors were used so that the maximum pressure gradient expected is close the maximum pressure gradient value measurable by the sensors. Permeability uncertainty is determined using uncertainties on the plug's geometry, fluids viscosities and pressure gradient. The final permeability uncertainty surrounds the different calculated uncertainties. The porosity determined through image processing using differential imaging ([7]) is 21.4%. An illustration of a cross-section of the mini plug is shown in Figure 2. The amount of the sub-resolved porosity (4%) represents approximately 19% of the total porosity, thus is low compared to the macro-porosity. Details on the reservoir rock characteristics are given in Table 2, and plots of porosity profiles (sub-resolved and macro porosity) are depicted in Figure 3.

Table 2. Sample characteristics.

Sample	D (mm)	L (mm)	K_w (D)	Φ_{total} (%)	Φ_{sub} (%)
Reservoir rock	10	15	4.65 +/- 0.4	21.9 +/- 0.5	~ 3.8

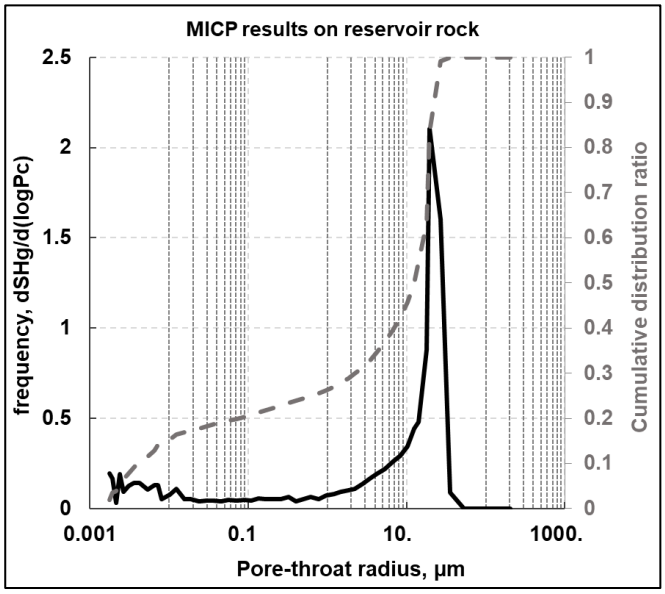

Fig. 1. Pore-throat radius size distribution and cumulative frequency of the reservoir rock determined through MICP experiments.

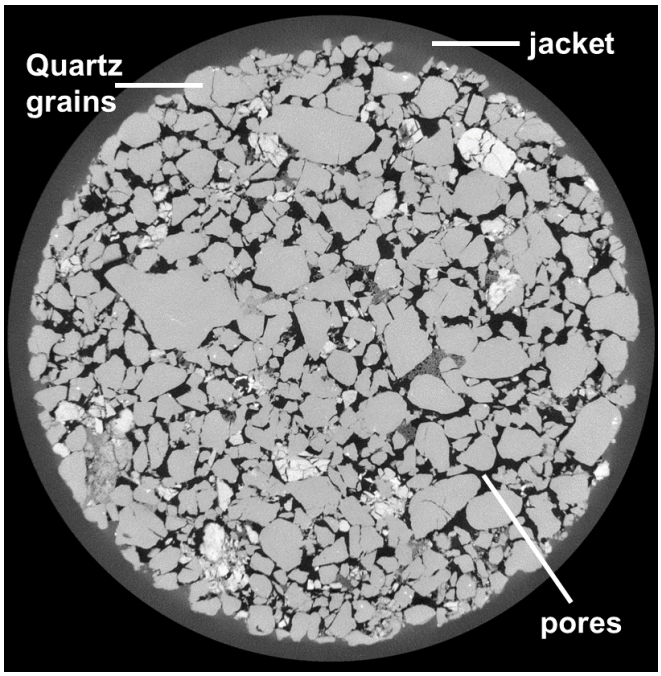

Fig. 2. Cross section of the 10mm dry reservoir rock at 5µm pixel resolution acquired on a Zeiss Versa 520 microtomograph.

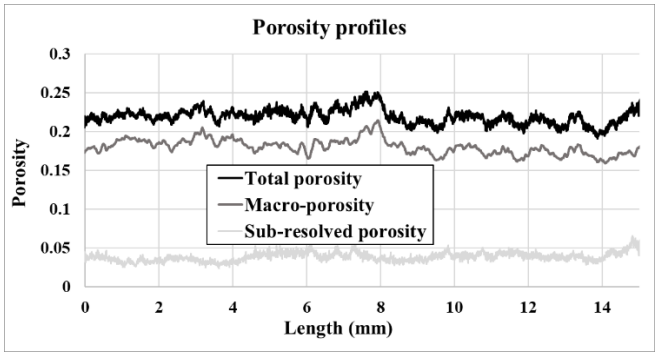

Fig. 3. Porosity profiles of the reservoir plug used in this study.

2.2. Fluids

In this study, two different brines were used for two distinct tests. We used an adapted reservoir formation brine (FB1) with no dopants, and an adapted formation brine (FB2) in which we added dopants (NaI). The reservoir formation brine (FB1) has a very low salinity, with a total amount of dissolved salt less than 13 g/l. When adding dopants, it is evident that the total dissolved solids resulting will be greater than that of the initial formation brine. Several tests were conducted to evaluate the minimal amount of dopants that needed to be added to the brine to have sufficient contrast between brine and oil without introducing significant uncertainties during image processing. These tests resulted in using at least 40 g/l of NaI. A third brine (FB3) composed of 300 g/l of NaI in distilled water was also used only to characterize the rock porosity through differential imaging. We used reservoir dead oil (DO) for the aging processes and mineral oil (Marcol 52) for displacement steps.

The compositions of the brines are given in Table 3 and fluids properties are given in Table 4 and in Table 5.

Table 3. Brines composition.

Salts	Formation brine (FB1) in g/l	Adapted brine (FB2) in g/l
NaI	0	40
NaCl	10.8	0
$CaCl_2+2H_2O$	0.25	0.25
MgCl2+6H2O	0.06	0.06
NaHCO3	1.5	1.46
KCl	0.1	0.11
Total	12.71	~ 42

Table 4. Fluids properties.

Fluids	T = 20°C		T = 90°C	
	ρ (g.cm^{-3})	**µ (cP)**	**ρ (g.cm^{-3})**	**µ (cP)**
FB1	1.12	1.39	1.1	0.48
FB2	1.15	1.32	1.12	0.46
Marcol 52	0.83	11.5	0.77	3.1
DO			0.86	2.6

Table 5. Dead oil characteristics.

Saturates	**Aromatics**	**Resins**	**Asphaltenes**	**TAN**	**TBN**
55.6%	35.8%	8.6%	1.8%	0.24	1.55

2.3. Image acquisition and processing

We utilized TotalEnergies' Zeiss Versa 520 microtomograph to acquire the 3D X-ray images. The energy and power settings were set at 90kV and 8W, respectively, and the voxel size was 5µm. With our 2000 x 2000 pixels camera, we were able to capture the entire sample diameter (10mm) in each scan. However, to cover the entire length (15mm), we required a total of 2 segments with an overlap between them. These segments were then stitched using a 3D reconstruction software resulting in a global 3D volume of the whole mini plug.

The image processing was conducted using Avizo 2023® and ImageJ softwares.

As previously mentioned, we employed a highly doped brine (300g/l NaI) for differential imaging processing to determine the macro-porosity and sub-resolved porosity profiles. However, for general flooding steps, we primarily utilized FB2. The main reason for this was to minimize the impact of the dopants on wettability alteration [6]. Consequently, the use of differential imaging for saturation tracking in the sub-resolved porosity was no longer feasible. To address this, we incorporated two new sets of 3D images: 100% fully saturated with M52 and 100% fully saturated with FB2. Subsequently, to track the saturation change within the sub-resolved porosity, we applied a linear interpolation of the histogram peak of the sub-resolved porosity between its maximum value (100% FB2) and its minimum value (100%

M52) after image normalization. This approach is presented in [8] and is illustrated in Figure 4.

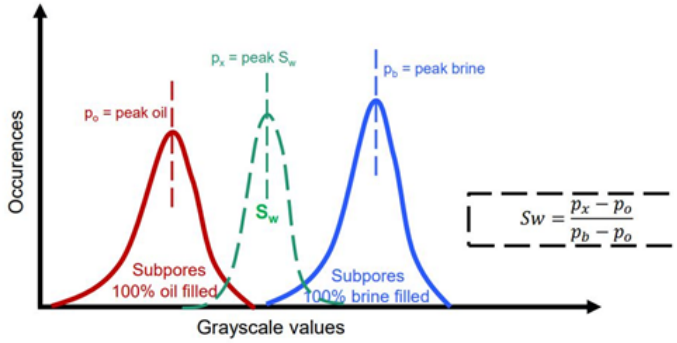

Fig. 4. Illustration of the linear interpolation to derive saturation in the sub-resolved porosity [8].

2.4. Old and new wettability anchoring experiments

The experimental set-up used in this study is similar to the one described by [1].

To evaluate the impact of dopants on wettability alteration, we conducted two different experiments on the same mini plug:

(i) The old wettability anchoring experiment followed the same steps as explained in [1]. For this first experiment, we used the doped formation brine (FB2), the mineral oil (M52) and for the ageing step, the dead oil (DO).

(ii) The new (upgraded) wettability anchoring experiment incorporated two brines (FB1 and FB2), a mineral oil M52, and dead oil (DO) for the aging process.

The targeted initial water saturation values (S_{wi}) for both experiments fall within the interval [13% - 16%]. Before each wettability anchoring experiment, the mini plug underwent intensive flow through cleaning known to be a good way of cleaning pore surfaces [9, 10]. We used sequences of toluene injection and a mixture of toluene (70%) - isopropyl alcohol (30%) at high temperature (90°C), followed by full injection of isopropyl alcohol and drying. The goal was to restore the sample's initial water-wet state.

Old wettability anchoring experiment (experiment 1): Firstly, we conducted a primary drainage by viscous flooding with M52 until reaching our S_{wi} target on the mini-plug initially fully saturated with FB2. It is crucial to carefully register the different flow rates used and the pressure gradients observed as they would be used as comparisons for the second experiment. After measuring flow properties at S_{wi} ($K_o(S_{wi})$), we replaced the mineral oil with toluene and then with dead oil under 90°C. Subsequently, the sample underwent aging for 1 month at 90°C, during which we injected a total of 10 pore volumes with a change of injection direction after 5 pore volumes to avoid any gradient on wettability distribution. After aging, $K_{ro}(S_{wi})$ was measured, and the temperature was decreased to 60°C. This was followed by the quick injection of 1 pore volume of toluene to replace the dead oil without significantly impacting the plug's wettability. Next, M52 was injected to replace toluene, and the temperature was decreased to ambient temperature. The Amott-like experiment could start. We first achieve a 2 weeks spontaneous imbibition phase using FB2 as explained in [1]. During this step, 2D images were taken punctually to monitor the capillary rise evolution of FB2 in the mini plug. This was followed by forced imbibition at increasing rates till a high rate (capillary number = 1E-05) to approach the residual oil saturation (Sor). Then followed a 2-week spontaneous drainage followed by forced drainage to complete the Amott-like experimental loop. For each step described above, the entire mini plug volume was scanned to draw average saturations, saturation profiles, and pore occupancies of the different fluids.

New wettability anchoring experiment (Experiment 2): The wettability anchoring experiment described above was upgraded to consider the recommendations highlighted by the experimental investigations from our SCAL laboratory [6]. The primary focus here was to perform the aging process using dead oil (DO) and FB1 instead of FB2. One particular challenge is the almost invisible contrast between FB1 and M52 or DO, making it impossible to quantify the saturation by image processing, whereas we needed quantitative information on saturations and statistics on pore occupancies. The experimental procedure is outlined as follows:

(1) After characterizing the mini plug petrophysical properties (such as porosity profiles, permeability), we conducted a primary drainage by viscous flooding with M52 on the mini plug fully saturated with FB2, using the same parameters as those used in the previous old wettability anchoring experiment (flow rates, pressure gradients, etc.), until reaching our S_{wi} target. $K_o(S_{wi})$ was checked to be close to that from the previous experiment (exp. 1). A full 3D image was acquired at the end of this step, and the pore occupancy of the brine was compared to that of the previous experiment to ensure similar brine distributions, thus ensuring the primary drainage wettability was the same.

(2) The plug was cleaned again and fully saturated with FB1. Permeability measurement was rechecked. After this, we conducted a primary drainage by viscous flooding using M52 and the same flow parameters as the previous primary drainage in (1) (flow rates, gradient pressures). At the end of this step, we checked that we obtained a similar $K_o(S_{wi})$ as before. A 3D image at this step was unnecessary as no contrast could be observed between brine and oil. However, it was assumed that we retained the same pore occupancy as observed in step (1) for similar $K_o(S_{wi})$, flow rates, and gradient pressures.

(3) M52 was replaced with toluene, then with dead oil under 90°C. This was followed by aging the sample for 1 month with the same protocol as described in the previous old wettability anchoring experiment. At this point, the recommendations of using formation brine and dead oil during aging [6] are followed.

(4) At the end of the aging process, $K_{ro}(S_{wi})$ with dead oil was measured, and then the temperature was decreased to 60°C. One pore volume of toluene was injected to replace dead oil, followed by 6 pore volumes of M52 to replace toluene. At the end of this step, the temperature was decreased to ambient temperature. At this point, no 3D acquisition was made as both FB1 and M52 present in the pore network had very low contrast.

(5) We initiate the spontaneous imbibition using the leaching process [1] at very low capillary number (8E-09) with **FB2** instead of FB1. There are two considerations here : (i) as shown by [6], a later injection of doped brine after a "correct" aging does not affect the plug's wettability much, (ii) if after aging, brine resides and is connected in clays and very small pores, which might generally be the case, diffusion between FB1 and FB2 will occur during the leaching process, and the brine present in the mini-plug after spontaneous imbibition will be closer to FB2 signal, allowing determination of saturations profiles and pore occupancies through image processing. During spontaneous imbibition, we monitored the rate of capillary rise of the brine, and after 2 weeks, we acquire an entire 3D image of the mini plug.

(6) After the spontaneous imbibition, we performed a forced imbibition with FB2 at increasing capillary numbers till a high capillary number (1E-05) to approach the residual oil saturation. It is followed with a reverse imbibition and an entire 3D image acquisition.

(7) After that, we perform a 2 weeks spontaneous drainage with M52 using the leaching process, followed by a forced drainage. In these steps, we used similar capillary numbers to the imbibition, and entire 3D images of the sample are always acquired.

The major benefit of the upgraded anchoring experiment is to provide a more reliable wettability output as direct reservoir fluids are used during aging. However, intuitively, one can already foresee that the new protocol is suitable for permeable rocks with a low amount of unresolved porosity and low values of S_{wi} to avoid a non-negligible impact of disconnected brine blobs due to wettability alteration.

3. Results and discussions

Experimental results will be divided into 4 sections: (i) Sample's initial states (S_{wi}), (ii) Spontaneous imbibition, (iii) Forced imbibition, (iv) Spontaneous and Forced drainage.

3.1 Sample's initial states (S_{wi})

It is essential that the sample's initializations at S_{wi}(s) exhibit the same state for both primary drainages in terms of pore occupancies, effective permeabilities, saturation profiles, and average values, after using the same primary drainage parameters (flow rates, gradient pressures, etc.). These states are expected to follow a water-wet trend, with brine in the smallest pores, clays, corners, and crevices, and oil in the larger pores. Similar average S_{wi} values were obtained in both experiments, 15.4% +/- 0.4% and 15.6% +/- 0.4% for exp.1 and exp.2, respectively.

For both experiments (exp.1 & 2), the final brine saturation is almost entirely trapped in the sub-porosity, with very low values encountered in the macro-porosity (<3%), thus within the segmentation uncertainty. Saturation profiles are illustrated in Figure 5. Effective permeabilities were both equal to the absolute permeability.

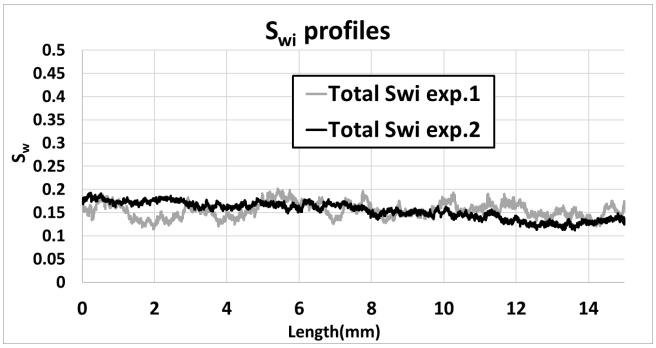

Fig. 5. Primary drainage saturation profiles before ageing.

With very close values of S_{wi}, similar pore occupancies and effective permeabilities at S_{wi}, we can attest that the two experiments' initial wettability and initial states are very similar.

3.2 Spontaneous imbibition

After ageing, we conducted 2 weeks of spontaneous imbibition for both experiments. The brine is injected and ejected from the bottom of the sample through a leaching process, the aim of which is to just contact the end face of the rock to initiate spontaneous infiltration into the rock. In the first few days, 2D static X-ray radiographies were acquired to monitor the capillary rise during spontaneous imbibition. The first 2D radiography image (system full of oil at S_{wi}) is subtracted from the subsequent 2D images, enhancing the visualization of the arrival of the doped brine (darker) and the capillary rise in the sample, as illustrated in Figure 6. The rise was at least twice as fast in experiment 1 than in experiment 2. The FB2 brine almost reached the top of the plug after 5 days in experiment 1, whereas it just nearly arrived at the top after 2 weeks for experiment 2. At this point, this confirms that the water-wet pores in which FB2 imbibed are more water-wet in experiment 1 (initial doped connate brine) than in experiment 2.

Comparison of saturation profiles illustrated in Figure 7 at the end of spontaneous imbibition also reveals more information.

(i) There is less brine imbibition in experiment 1 than in experiment 2, with quicker imbibition in experiment 1 than in experiment 2.

(ii) In experiment 2, we observed that the sub-porosity grayscale signal increased. Its saturation was found to be computable (see Figure 7) and almost equal to that after primary drainage. It means the FB2 used for spontaneous imbibition has totally diffused in the connate brine (FB1) initially in the sub-pores, and also that brine remained totally connected within sub-pores. For both experiments, the saturation profile in the sub-porosity remains almost equivalent stating that the sub-porosity remained water-wet in both experiments.

(iii) The main saturation difference occurs in the macro-porosity, where we have almost 10% of difference (see Table 6).

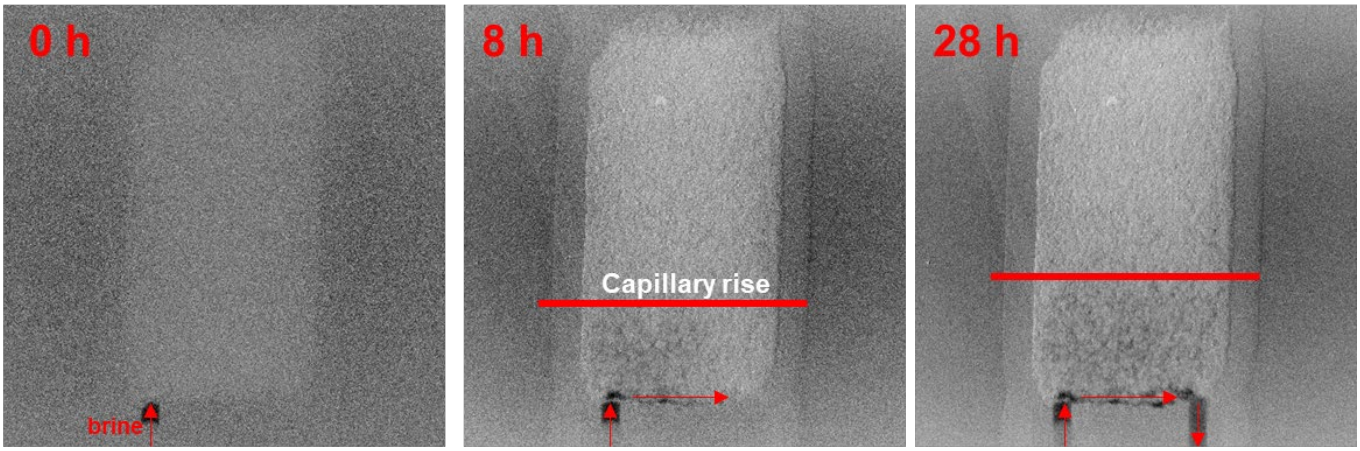

Fig. 6. Monitoring of the capillary rise of FB2 (doped brine) during spontaneous imbibition. The brine (darker phase) arrives from the left hole and goes out from the right hole.

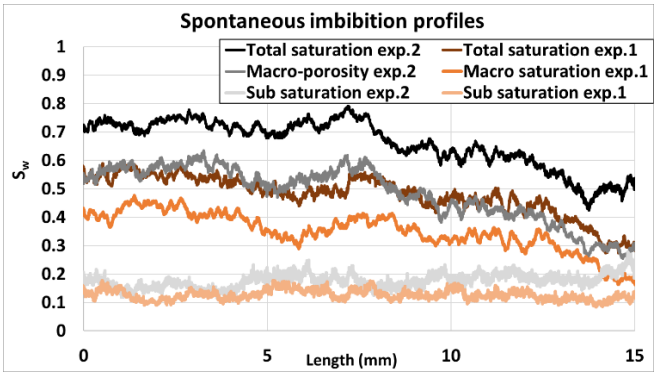

Fig. 7. Saturation profiles after the spontaneous imbibition step of experiment 1 & 2.

Differences in imbibed brine volumes occurred during both experiments. The rate of the capillary rise differs, and water-wet pores tend to remain more water-wet, i.e., with lower advancing contact angles, when the connate brine is doped. But counter-intuitively, we observed that a more important brine volume imbibed for experiment 2 where the connate brine is the formation brine. One possible explanation is that the high rate of capillary rise in experiment 1 generates trapping by bypass or snap-off of oil in pores. Pores imbibed with brine are water-wet. But in this trapping configuration, pores filled with oil are not necessarily oil-wet because they could have been bypassed, or oil can be trapped by snap-off with brine contacting the pore walls only by layer films. A lower rise rate (higher advancing contact angles) as in experiment 2 may be more efficient in displacing oil with much lower trapping than in experiment 1.

Table 6. Average brine saturations after the spontaneous and the forced imbibition steps.

Step	Spontaneous imbibition		Forced imbibition	
experiment	exp.1	exp.2	exp.1	exp.2
Total Sw (%)	46.9	66.2	71.7	81.3
Sw av. in sub (%)	12.7	17.7	12.7	17.7
Sw av. in macro (%)	34.2	48.5	59	63.6

Another important information that can be drawn from spontaneous imbibition experiments is the wettability model, given by the correlation of the imbibed pores with pore radii. It was used by [1, 2] as one of the main inputs in PNM simulations to predict reliable relative permeabilities. Some authors [11] proposed 3 models: Fractional-wet, Mixed-wet small and mixed-wet large models.

Pore networks of around 1500 x 1500 x 1000 voxels have been extracted from the images using the pore network extraction code called GNextract developed with Imperial college of London [12]. We isolated the water-wet imbibed pores, and we plotted their volumetric fraction as a function of the pore radii in Figure 8 for both exp.1 & 2.

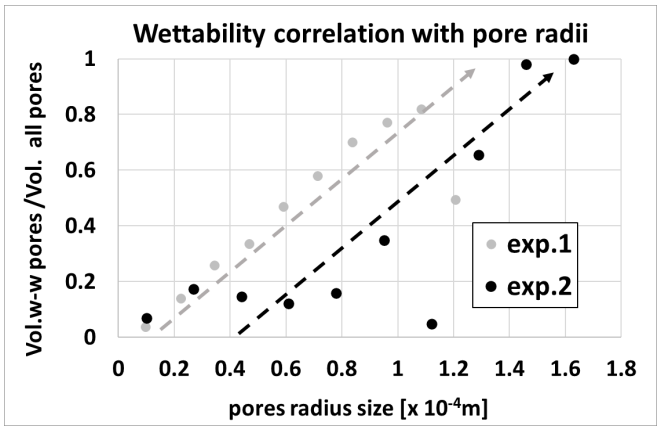

Fig. 8. Wettability correlation with pores radii for exp. 1 & 2.

The same trend is observed in both experiments with large pores systems more likely to be imbibed by brine than small pores, typically a Mixed-Wet Small (MWS) model. Thus, the same wettability model is valid for both experiments.

3.3 Forced imbibition

Waterflooding is first performed vertically from bottom to top with increasing capillary numbers (C_a) until 1E-05. Each flow rate is maintained until constant pressure drop (DP) is reached. After the highest C_a step, the flow injection is reversed, and the maximum C_a is directly applied to flatten saturation profiles. Figure 9 illustrates final saturation profiles obtained after waterflooding processes. Average saturations are listed in Table 6.

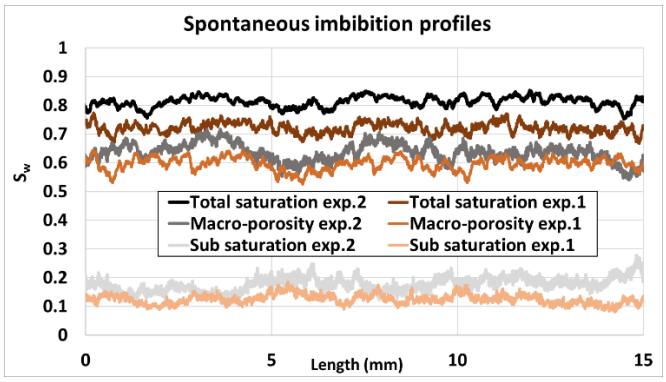

Fig. 9. Saturation profiles after forced imbibition in exp. 1 & 2.

Brine saturation does not change anymore in the sub-porosity for both experiments. We observe more trapping of oil in macropores for exp.1. It emphasizes the possibility of partial oil trapping that might have occurred during spontaneous imbibition more in exp.1 than in exp.2. There is almost 10 p.u difference in remaining oil saturation between both experiments.

3.4 Spontaneous & Forced drainage

Drainage steps are achieved using the mineral oil M52, respecting density contrast, by injecting oil from the top of the plug.

For the spontaneous process, we used the 2-week leaching process, where oil contacts the plug at the top end and leaves the system at the same top end. A very low capillary number is used in this process (1E-09). After 2 weeks, we performed forced drainage where oil flows through the sample from top to bottom with increasing capillary numbers until the maximum DP that was achieved during primary drainage. After that, we reverse the flow direction at the maximal capillary number obtained to flatten the saturation profiles.

Spontaneous drainage saturation profiles from exp.1 & 2 are compared with forced imbibition profiles in Figure 10. Average values are given in Table 7.

Table 7. Average saturations during Forced imbibition and spontaneous drainage.

Step	Forced imbibition		Spontaneous drainage	
Experiment	exp.1	exp.2	exp.1	exp.2
Total Sw (%)	71.7	81.3	67.3	81.8
Sw av. in sub (%)	12.7	17.7	12.5	17.7
Sw av. in macro (%)	59	63.6	54.8	64.1

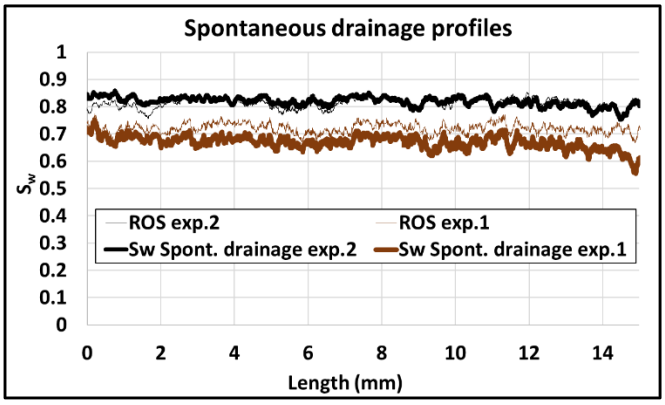

Fig. 10. Comparisons between Forced imbibition and spontaneous drainage saturation profiles from exp. 1 & 2.

We observed a small amount of spontaneous drainage in exp.1 with oil saturation slightly increasing across the sample's total length after 2 weeks only within the macro-porosity. This general increase is only possible by connected oil-wet pores. We did not observe any spontaneous drainage for exp.2. Still, exp.2 could have a few oil-wet pores, but these oil pores would be disconnected.

Forced drainage experiment led to almost the same values of S_{wi} (see Figure 10) than that from primary drainage, with slightly higher values. These increases are mainly located in the macro-pores and remain within the uncertainties of saturation calculations.

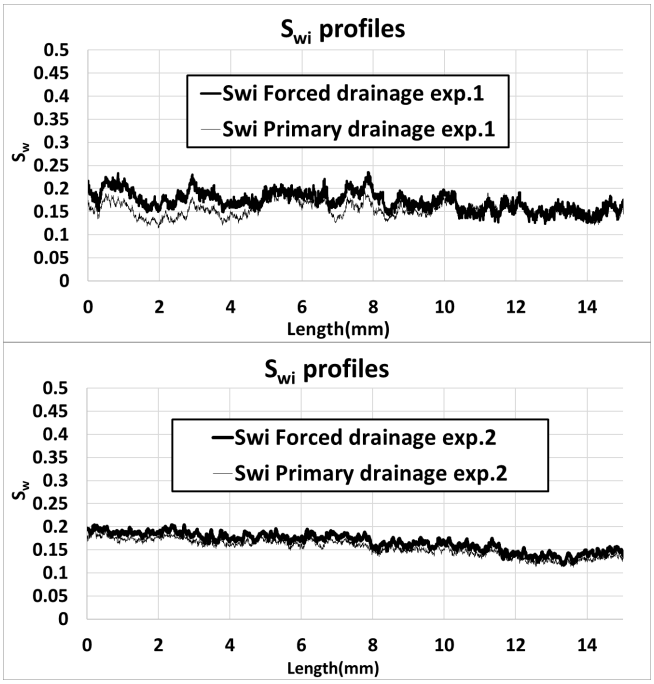

Fig. 11. Comparisons of Swi between primary drainage and second (forced) drainage for exp.1&2.

4. Conclusions and perspectives

Two different wettability anchoring experiments were performed on the same sample, starting with the same water-wet state with almost the same values, profiles and pore occupancies of S_{wi}, and identical flow parameters used

throughout the studies. The only difference between both experimental protocols is the ageing process, achieved with a doped connate brine for exp.1 and with a non-doped connate brine for exp.2. Many differences were observed, highlighting the real importance of addressing the issue of non-representative wettability on multiphase flow properties when using dopants in fluids. Despite having the same MWS wettability model in both experiments, we observed:

(1) Different spontaneous imbibition rates, with faster capillary rise through water-wet pores when dopants are used. Water-wet pores have lower advancing contact angles in exp.1 than in exp.2.

(2) Significant differences in the amount of imbibed brine volumes, possibly due to the impact of the wettability degree and trapping caused by the capillary rise rate.

(3) Differences in residual oil saturations, with the highest value achieved on exp.1 where dopants are used for ageing.

(4) Spontaneous drainage observed in exp.1 and not in exp.2. There were some oil-wet pores connected in exp.1 which was not the case for exp.2.

These significant differences highlight the fact that the new wettability anchoring protocol, driven by recommendations from our SCAL laboratory, contributes to providing more reliable and robust wettability inputs for PNM simulations. Nevertheless, the new protocol still has some limitations: (i) for samples with a non-negligible amount of sub-porosity, saturation computation can be challenging if oil migrates into sub-pores during ageing, (ii) If brine becomes trapped in the center of pores after ageing as observed in [1], disconnected brine will not participate in saturation computation, potentially biasing saturation determination, (iii) the protocol is more time-consuming in both experiments (two primary drainages) and interpretation (saturation tracking is challenging).

A possible future direction for this study is to investigate dopants in oil instead of brine. For example, a small fraction of Iododecane can be used in mineral oil to enhance the contrast between oil and non-doped brine. This could simplify the experimental process by:

(i) Reducing the experimental processes with achieving only one primary drainage: where primary drainage is directly performed using the doped mineral oil and non-doped brine. Saturation computations are straightforward due to the good contrast between the doped oil and non-doped brine.

(ii) Enabling the implementation of ageing following recommendations from [6]: After primary drainage, the doped mineral oil is directly replaced by toluene and then by dead oil. This leads to the ageing step being directly performed using dead oil and non-doped brine as needed.

(iii) Increasing the reliability of saturation tracking in porosity after ageing: After ageing processes, the most representative and well-connected fluid in the sample is dead oil. Injecting 1PV of decalin to displace the dead oil, followed by multiple PVs of doped oil to replace decalin, would allow for quantitative tracking and visualization of the brine, owing to the good contrast between brine and doped oil.

Using dopants in mineral oil addresses the limitations of the current upgraded protocols. An experimental investigation is then needed to understand if using doped oil after ageing does not alter the plug's wettability during post-ageing steps.

We thank TotalEnergies for their financial support and the permission to publish this paper.

5. References

1. Regained M, Nono F, Farhana Faisal, Titly, Rivenq Richard. Large Pore Network simulations coupled with innovative wettability anchoring experiment to predict relative permeability of a mixed-wet rock. Transport in Porous Media, (2022).

2. Regaieg M, Farhana Faisal, Titly, Nono F, Pairoys F, Fernandes V and Caubit C. Prediction of relative permeability and fast wettability assessment using Digital Rock Physics: An operational study on a Reservoir Sandstone. SCA2023-26, (2023).

3. Jadhunandan, P.P., Morrow, N.R.; Effect of wettability recovery for crude oil/brine/rock system, SPE 22597, (1995).

4. Stock, P., Muller, M., Utzig, T., Valtiner, M.; How specific halide adsorption varies hydrophobic interactions, A Journal of Biomaterials and Biological Interfaces. 11, 019007, (2016).

5. Al-Hamad, M., Al-Zoukani, A., Ali, F., Badri, M., Abdallah, W.; Dynamic waterflooding in carbonates: the role of iodide ions SPE 188026, (2017).

6. Pairoys, F., Caubit, C., Rochereau, L., Nepesov, A., Danielczick, Q., Agenet, N., Nono, F.; Impact of Dopants on SCAL Experiments, Phase I; SCA2023-007, (2023).

7. Q. Lin, Y. Al-khulaifi, B. Bijeljic and M.J. Blunt, 'Quantification of sub-resolution porosity in carbonate rocks by applying high-salinity contrast brine using Xray microtomography differential imaging', Advances in Water Resources. 96. 10.1016/j.advwatres.2016.08.002, (2016).

8. Fernandes, V., Nono, F., Nicot, B., Pairoys, F., Bertin, H., Lachaud, J., Caubit, C. ; Hybrid Drainage Technique application on bimodal limeston ; SCA2023-006, (2023).

9. Ma, S. M., Belowi, A., Pairoys, F., Ahmad, Z.: Quality assurance of carbonate rock special core analysis – lesson learnt from a multi-year research project, IPTC, Beijing, China, (2013).

10. Qatari, H. A., Ma, S. M., Hafez, A., Okashah, T. : Core cleaning for wettability restoration – how clean is clean ?, SPWLA 65th Annual Logging Symposium, Rio de Janeiro, (2024).

11. Dixit AB, Buckley JS, McDougall SR, Sorbie KS. Empirical measures of wettability in porous media and the

relationship between them derived from pore-scale modelling. Transport in Porous Media, 40(1):27–54, (2000).

12. A.G. Raeini, B. Bijeljic, M.J. Blunt: Generalized network modeling of capillary-dominated two-phase flow. Physicalreview.E97(21),23308(2018).Doi:10.1103/Phys RevE.97.023308F. De Lillo, F. Cecconi, G. Lacorata, A. Vulpiani, EPL, 84 (2008).